CDF/PUB/EXOTIC/PUBLIC/8070
Version 1.0
January 27, 2006

CDF's Higgs Sensitivity Status[1]

Tom Junk

University of Illinois at Urbana-Champaign
on behalf of the CDF Collaboration

Abstract

The combined sensitivity of CDF's current Standard Model Higgs boson searches is presented. The expected 95% CL limits on the production cross section times the relevant Higgs boson branching ratios are computed for the $W^{\pm}H \to \ell^{\pm}\nu b\bar{b}$, $ZH \to \nu\bar{\nu}b\bar{b}$, $gg \to H \to W^+W^-$ $W^{\pm}H \to W^{\pm}W^+W^-$ channels as they stand as of the October 2005, using results which were prepared for Summer 2005 conferences and a newer result form the $gg \to H \to W^+W^-$ channel. Correlated and uncorrelated systematic uncertainties are taken into account, and the luminosity requirements for 95% CL exclusion, 3σ evidence, and 5σ discovery are computed for median experimental outcomes. A list of improvements required to achieve the sensitivity to a SM Higgs boson as quantified in the Higgs Sensitivity Working Group's report is provided.

1 Introduction

The search for the Standard Model (SM) Higgs boson is one of the central pieces of the current High Energy Physics program. The $SU(2) \times U(1)$ gauge model of electroweak interactions makes a number of predictions which have been experimentally verified to high precision, but its validity depends on the breaking of this symmetry to the $U(1)_{\rm EM}$ symmetry group at low

[1]Presented at the TeV4LHC Workshop, October 21, 2005

energies. Many differing proposals of the details of this symmetry breaking have been advanced, most of which predict one or more observable scalar bosons. If the minimal SM Higgs mechanism describes nature, then precision electroweak data [1] provide evidence that the scalar Higgs boson should be lighter than about 200 GeV, with a preferred value at around 115 GeV. Direct searches at LEP have excluded [2] a SM Higgs boson with a mass below 114.4 GeV. If there is a SM Higgs boson with a mass between $\sim$ 115 GeV and $\sim$ 200 GeV it is produced in $p\bar{p}$ collisions at the Tevatron, and, with enough data, it should be possible to exclude or discover such a particle.

Data are being accumulated by the Tevatron experiments CDF and DØ, whose runs are expected extend until 2009. Currently, more than 1 fb^{-1} of data have been recorded by each experiment, although the Higgs boson searches reported here are based on approximately 300 pb^{-1} of data. With 300 pb^{-1} of data and the expected signal-to-background ratios in the channels, the SM Higgs boson hypothesis cannot be tested for any value of m_H. Nonetheless, with additional data, and improvements to the analyses, sensitivity at the 95% CL level may be obtained for m_H up to 180 GeV, assuming the design integrated luminosity of 8 fb^{-1} is collected with good quality by both detectors, according to a 1999 study [3]. An updated study [4] was conducted in 2003 to check the earlier projections with more realistic simulations and preliminary data samples which could be used to calibrate some backgrounds. The later study did not consider searches for Higgs bosons with m_H greater than 130 GeV, and also did not include the effects of systematic uncertainties on the amount of luminosity required to test for Higgs bosons. Each report includes calculations of the estimated amounts of luminosity required for a combination of all of CDF's channels and DØ's channels to exclude at the 95% CL, assuming a Higgs boson is not present, as well as the luminosity requirements for a combined 3σ evidence and 5σ discovery. The luminosity thresholds are shown in Figure 1 for the 1999 study and in Figure 2 for the 2003 study.

The CDF channels as they stand as of the Summer 2005 conferences are not as powerful as those assumed in the two sensitivity studies. The following sections provide a snapshot of the sensitivity of the CDF channels separately and combined, as of the October 2005 TeV4LHC workshop, with plans for improvement.

2 Sensitivity by Channel

The expected signal and background rates and shape distributions were collected from each of the channel analysis teams and combined using the CL_s technique [10] to find the expected limits on the cross-section multiplied by the branching fractions. Candidate information was not included in the combination, so the observed limit of the combination is not computed. All of the observed limits in the channels are close to expectations, the observed limit of the

combination is expected to be close to the expected combined limit.

2.1 The $W^{\pm}H \to \ell^{\pm}\nu b\bar{b}$ Channel

The results of the $W^{\pm}H \to \ell^{\pm}\nu b\bar{b}$ search are described in [5]. The reconstructed mass distribution in the single-tagged analysis is used in computing the expected limits, with each bin counted as an independent counting experiment. Systematic errors are taken on the background and signal rates, but the shapes are not varied. Each bin is assumed to have fully correlated systematic uncertainties with all other bins of the mass distribution. The systematic uncertainties are detailed in Table 2. Acceptances and signal distributions are linearly interpolated [11] between the supplied test points at which Monte Carlo samples are available. The observed and expected cross-section times branching ratio limits are shown at the 95% CL in Figure 3 as a function of m_H.

2.2 The $ZH \to \nu\bar{\nu}b\bar{b}$ Channel

The results of the $ZH \to \nu\bar{\nu}b\bar{b}$ search are described in [6]. The reconstructed mass distribution was not provided for combination, but the numbers of events for the expected signal and background after a mass window cut which moves with the Higgs boson mass under test are used. They are linearly interpolated between the model points listed in [6]. The systematic uncertainties on the signal and background are detailed in Table 2. The observed and expected cross-section times branching ratio limit is shown at the 95% CL in Figure 4 as a function of m_H, and compared to the SM expectation.

2.3 The $ZH \to \ell^+\ell^-b\bar{b}$ Channel

The $ZH \to \ell^+\ell^-b\bar{b}$ channel is still in development and the analysis is still in its "blind" stage. Hence, data candidate information is not yet available. The current status is described in [9]. The selection starts with a very clean sample of $Z \to \ell^+\ell^-$ decays, identifying isolated leptons with $m_{\ell\ell}$ close to m_Z, and two or three jets, at least one of which must be b-tagged. The systematic uncertainties on the signal and background are detailed in Table 2. The neural net has seventeen input variables described in [9]. The most powerful ones are the invariant mass of the two leading jets taken together, the event H_T (which is the scalar sum of all the P_T's of the observed particles), and the E_T of the leading jet. The median expected limit on the cross-section times the branching ratio for this process is approximately 2.2 pb for 300 pb^{-1} of data. This expected limit is lower than that for other channels mainly due to the very small background prediction. It must be compared, however, against a much smaller SM signal

expectation.

2.4 The $gg \to H \to W^+W^-$ Channel

The results of the $gg \to H \to W^+W^-$ search are described in [7]. The histograms of $\Delta\phi_{\ell\ell}$ are used as the discriminant variable input to the limit calculation – each bin is a separate counting experiment. The shapes are interpolated [11] between m_H points, as are the signal rates and background rates. The analysis uses m_H-dependent cuts, and so the background rates depend on the m_H under test. The systematic uncertainties on the signal and background are detailed in Table 2.

The median expected 95% CL cross-section times branching ratio limit is shown in Figure 6 as a function of m_H compared to the SM expectation and to the computation of [7].

2.5 The $W^{\pm}H \to W^{\pm}W^+W^-$ Channel

The results of the $W^{\pm}H \to W^{\pm}W^+W^-$ search are described in [8]. It is a single counting experiment – there are no discriminant variables whose histograms have different s/b ratios to use. The acceptance is interpolated between the m_H points listed in [8]. The systematic uncertainties on the signal and background are detailed in Table 2. For this calculation, the data statistical uncertainty on the residual conversion background is treated as independent of the other errors on the background and the errors add in quadrature instead of linearly as they do in [8]. Furthermore, the FSR systematic uncertainty is almost certainly truly uncorrelated with other channels' FSR uncertainty, but it has been treated as correlated. As is seen below, the entire systematic error treatment in this channel matters little to the sensitivity.

The observed cross-section times branching ratio limit is shown at the 95% CL in Figure 7 as a function of m_H compared to the SM expectation and to the computation of [8].

3 Sensitivity of the SM Channels when Combined

The observed 95% CL limits in all of CDF's SM Higgs channels are shown, compared with SM predictions, and also compared with observed limits from DØ's channels, in Figure 8. The different searches search for different processes which have different rates, and thus contribute differently to the combined sensitivity. It is somewhat easier to compare the channels' sensitivity to a SM Higgs when the ratio of the limit in each channel to the SM prediction is formed. This ratio is shown for the same collection of CDF and DØ channels in Figure 9.

The CL_s method is used on the collection of CDF's five SM Higgs boson search channels to

compute the multiplicative scale factor s_{95} on the total signal which can just barely be expected to be excluded in a median experimental outcome. This procedure doesn't make much physical sense for scale factors exceeding unity, as there isn't a well-motivated physical model which scales all of the production mechanisms for SM Higgs bosons in the same way, but it provides a technical benchmark of how far we are from the SM in our sensitivity. The results of this combination are shown in Figure 10. It must be shown as a multiplicative factor of the SM prediction because of the different SM predictions used for each search channel.

4 Necessary SM Channel Improvements

The current channels as we have them are insufficient to test for the presence or absence of the Standard Model Higgs boson, even if the projected 8 fb^{-1} of data are collected. Improvements must be made to increase the acceptance, reduce the background, and to separate the selected events into disjoint subsets with different s/b ratios, and to combine them together. Furthermore, the results must be combined with DØ.

The Higgs Sensitivity Working Group report [4] lists changes which can be made to the analyses which can get us to the desired level of sensitivity. Much of this work has already been done to improve our resolutions, to increase our lepton acceptance to the forward region, and to develop neural nets. But the work has been done by a variety of different people separated in space, time, and institution. The work of many groups must be collected together in the analysis channels in order to achieve the sensitivity reported in [3, 4].

The factors on the expected amount of luminosity needed to get exclusion at the 95% CL, 3σ evidence and 5σ discovery can be computed for most of the improvements rather easily. For acceptance increases, the background ought to increase as the signal acceptance increases. In fact, it should increase faster, because as we expand our acceptance to forward regions of the detector or to include leptons of lower quality, a larger fraction of background is expected to creep in. For this estimation, the estimations are taken from the HSWG report's Sections 2.3 and 4.2 (for the Neural Net factor). A listing of improvements and their factors in luminosity is given in Table 3. It is assumed in the luminosity projections that the systematic uncertainties will scale inversely with the square root of the integrate luminosity. Furthermore, accounting of the shape uncertainties may make the systematic errors larger.

The neural net factor of 1.75 is not uniformly applicable to all channels, as the $ZH \to \ell^+\ell^- b\bar{b}$ channel estimations already take advantage of a neural net. The forward lepton acceptance improvement cannot strictly be multiplied by the track-only lepton factor since the forward tracking is not sufficient. Nonetheless, a naive product of the factors from the analysis improvements is approximatley 20. The analysis improvements will not be made all at once – work is ongoing to develop and characterize the techniques.

5 SM Sensitivity Projections

Assuming that the acceptances of the channels are increased and neural nets or other advanced techniques are used to reduce the backgrounds, the projected reach of of the Tevatron SM Higgs search program is estimated. It is assumed that the systematic uncertainties scale inversely with the square root of the integrated luminosity, and that DØ contributes channels with the same sensitivity as CDF's and that they are combined together. Figure 11 shows how the significance of an excess of events is expected to develop, as a function of the integrated luminosity collected per experiment, assuming a SM Higgs boson is present with a mass $m_H = 115$ GeV. The actual evolution of such an excess, if a signal is actually present, will be more of a random walk as data are collected, so the figure also includes the width of the expected distribution. Figure 12 shows the evolution of the probability of seeing a 2σ, a 3σ, or a 5σ excess in the combined data when searching for a SM Higgs boson of mass $m_H = 115$ GeV, if it is truly present, as a function of the luminosity collected by each experiment. After collecting 8 fb^{-1} per experiment, it is 10% likely that a 5σ excess will be observed if m_H is truly 115 GeV.

6 The MSSM $H/h/A \to \tau^+\tau^-$ Sensitivity

CDF has published its search for $H/h/A \to \tau^+\tau^-$ search, using 310 pb^{-1} of Run 2 collision data. Tau pairs are selected in which one tau decays leptonically, and the other decays semi-hadronically. Kinematic selection requirements were designed to separate tau pairs from W+jets and QCD backgrounds, in which jets are misidentified as taus. The dominant remaining background is $Z \to \tau^+\tau^-$ production. In order to separate $H/h/A \to \tau^+\tau^-$ from this and other backgrounds, the invariant mass of the visible tau decay products is formed, shown in Figure 13. The reconstructed invariant mass of Higgs boson signal events peaks near the signal mass, with a width which grows rapidly with increasing Higgs boson signal mass. This is offset by the fact that the background is very small for large reconstructed masses. The observed and expected limits on the production cross section times the decay branching ratio to tau pairs is shown in Figure 14.

This cross-section limit can be interpreted in the MSSM; we choose to represent it as an exclusion in the $(m_A, \tan\beta)$ plane in the $mh-max$ and $no-mixing$ MSSM benchmark scenarios [13]. This interpretation benefits from the fact that for larte $\tan\beta$, two Higgs bosons (either h and A, or H and A), are nearly degenerate in mass and contribute rougly equally to the expected signal. CDF's observed 95% CL limits are shown in Figure 15, along with projected CDF+DØ combined sensitivity contours for 2, 4, and 8 fb^{-1} of data collected by both CDF and DØ. The large improvement in sensitivity at larger Higgs boson masses comes from the fact that the background rate is very low for large invariant-mass tau pairs. For a search with a

large background rate, the expected signal limit is roughly inversely proportional to the square root of the integrated luminosity, while for searches with very small backgrounds, the expected limit is roughly inversely proportional to the integrated luminosity.

References

[1] The ALEPH, DELPHI, L3 and OPAL Collaborations, and the LEP Electroweak Working Group, `ArXiv:hep-ex/0511027` (2005).

[2] The ALEPH, DELPHI, L3 and OPAL Collaborations, and the LEP Higgs Working Group, Phys. Lett. **B 565** 61–75 (2003).

[3] M. Carena, J. Conway, H. Haber, J. Hobbs *et al.*, "Report of the the Higgs Working Group of the Tevatron Run 2 SUSY/Higgs Workshop", `ArXiv:hep-ph/0010338` (2000).

[4] J. Kroll, B. Winer *et al.*, "Results of the Tevatron Higgs Sensitivity Study", CDF Note 6353, FERMILAB-PUB-03-320-E (2003).

[5] CDF Collaboration, CDF Note 7740 (2005). The results and this note are available on CDF's public results web page `http://www-cdf.fnal.gov/physics/exotic/exotic.html`.

[6] CDF Collaboration, CDF Note 7983 (2005) This note is available on CDF's public results page `http://www-cdf.fnal.gov/physics/exotic/exotic.html`.

[7] CDF Collaboration, CDF Note 7893 (2005). This note is available on CDF's public results page `http://www-cdf.fnal.gov/physics/exotic/exotic.html`.

[8] CDF Collaboration, CDF Note 7307 (2004). This note is available on CDF's public results page `http://www-cdf.fnal.gov/physics/exotic/exotic.html`.

[9] J. Efron, "Search for Higgs Boson Production via the Process $p\bar{p} \to ZH \to l^+l^-b\bar{b}$ at CDF", presented at the APS/DPF April Meeting, Tampa, Florida, April 16–19, 2005.

[10] A. Read, J.Phys.G28:2693-2704 (2002)
T. Junk Nucl. Instrum. Meth. **A434** 435 (1999).

[11] A. Read, Nucl. Instrum. Meth. **A425** 357-360 (1999).

[12] A. Abulencia *et al.* [CDF Collaboration], Phys. Rev. Lett. **96**, 011802 (2006) [arXiv:hep-ex/0508051]. Additional description and figures are available at `http://www-cdf.fnal.gov/physics/exotic/exotic.html`.

[13] M. Carena, S. Heinemeyer, C. E. M. Wagner and G. Weiglein, arXiv:hep-ph/9912223. Eur. Phys. J. **C** 26, 601 (2003).

Table 1: Integrated luminosities by channel.

Channel	$\int \mathcal{L}dt$ (pb^{-1})	Reference
$W^{\pm}H \to \ell^{\pm}\nu b\bar{b}$	319	[5]
$ZH \to \nu\bar{\nu}b\bar{b}$	289	[6]
$gg \to H \to W^{+}W^{-}$	360	[7]
$W^{\pm}H \to W^{\pm}W^{+}W^{-}$	194	[8]

Table 2: Relative systematic uncertainties by channel. Errors from the same source are considered correlated, across channels, and between signal and background. The "uncorrelated" errors are uncorrelated across channels and between signal and background.

	Channel									
	$W^{\pm}H \to \ell^{\pm}\nu bb$		$ZH \to \nu\bar{\nu}bb$		$ZH \to \ell^{+}\ell^{-}b\bar{b}$		$gg \to H \to W^{+}W^{-}$		$W^{\pm}H \to W^{\pm}W^{+}W^{-}$	
Source	s [%]	b [%]	s [%]	b [%]	s [%]	b [%]	s [%]	b [%]	s [%]	b [%]
lumi	6	6	6	6	6	6	6	6	6	6
b-tag s.f.	5		6.4	1.9	15	15			0.37	
lepton ID	5				7	7				
lepton trig	0.6				1	1			2.4	
PDF	1								1.5	
ISR	3								3.0	
FSR	7				7				3.2	
JES	3		7.8	3.5						
Jet model	1.4									
$\nu\nu b\bar{b}$ trig			3	1.5						
$\nu\nu b\bar{b}$ veto			2	2						
uncorrelated		15	2	22.1		9	6	7	3.7	66

Table 3: Luminosity factors expected from analysis improvements, separated by channel.

Improvement	$W^{\pm}H \to \ell^{\pm}\nu b\bar{b}$	$ZH \to \nu\bar{\nu}b\bar{b}$	$ZH \to \ell^{+}\ell^{-}b\bar{b}$
m_H Resolution	1.7	1.7	1.7
Continuous b-tags	1.5	1.5	1.5
Forward B-tags	1.1	1.1	1.1
Forward Leptons	1.3	1.0	1.6
Neural Nets	1.75	1.75	1.0
Track-Only Leptons	1.4	1.0	1.6
WH signal in ZH	1.0	2.7	1.0
Product of above	8.9	13.3	7.2
CDF+DØ Combination	2.0	2.0	2.0
All Combined	17.8	26.6	14.4

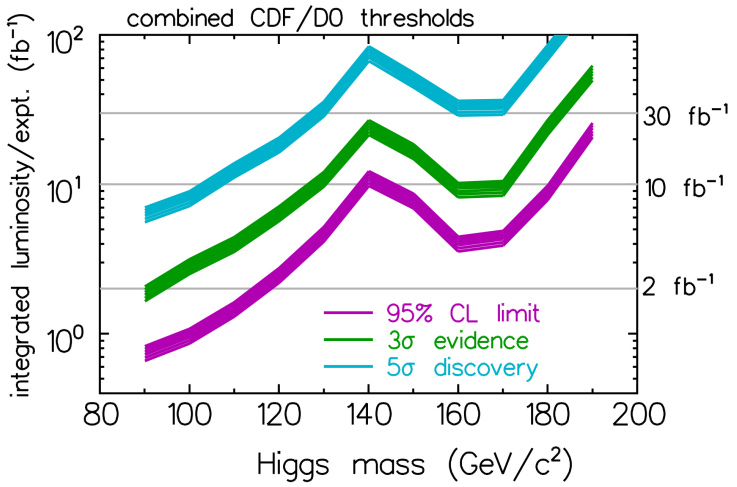

Figure 1: SUSY/Higgs Working Group estimations of the luminosity required for 95% exclusion, 3σ evidence, and 5σ discovery for the combined CDF+DØ search channels. (2000).

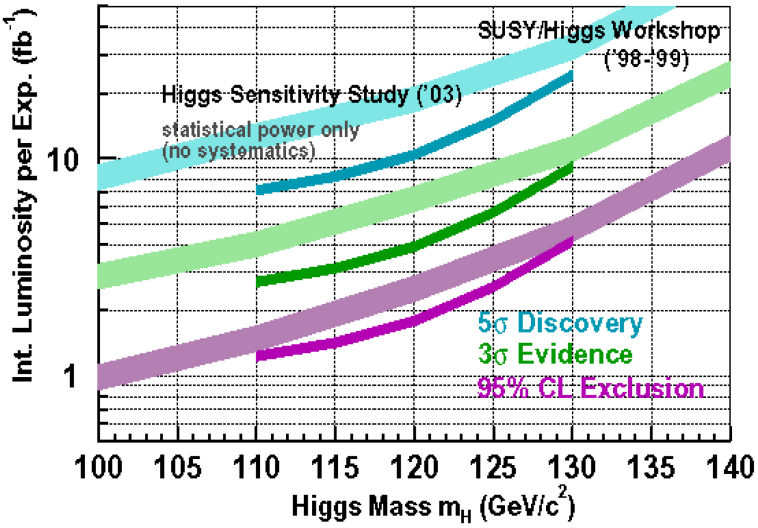

Figure 2: Higgs Sensitivity Working Group estimations of the luminosity required for 95% exclusion, 3σ evidence, and 5σ discovery for the combined CDF+DØ search channels, compared against the earlier SUSY/Higgs Working Group's calculation.

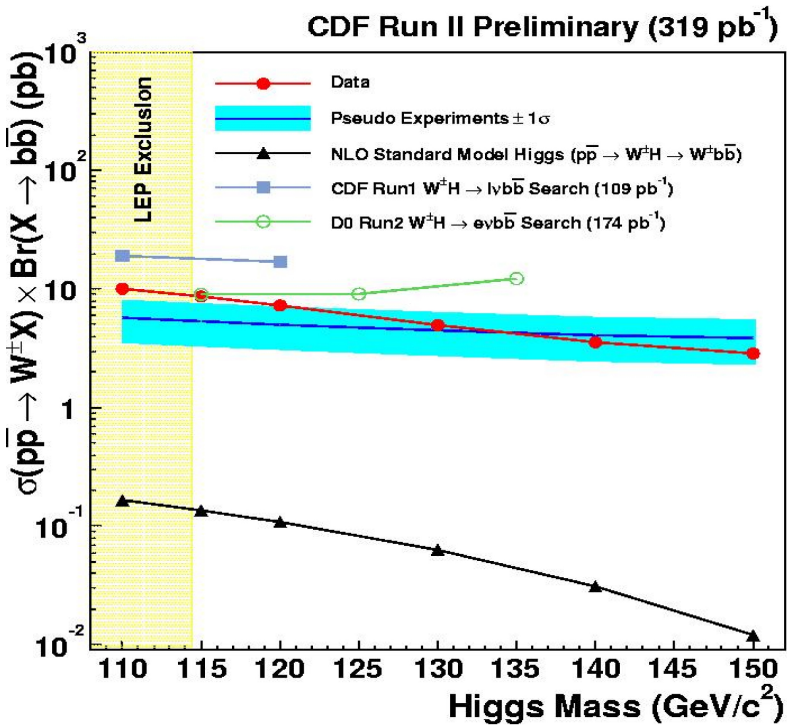

Figure 3: The observed and expected 95% CL limits on the production cross-section times the Higgs decay branching ratio as a function of m_H for the $W^{\pm}H \to \ell^{\pm}\nu b\bar{b}$ channel. The limits are compared with the SM prediction.

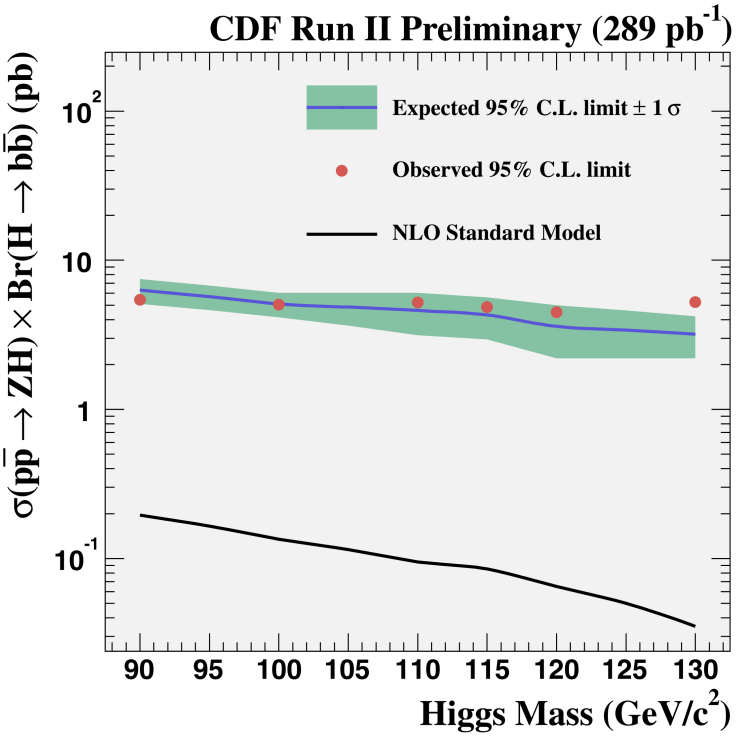

Figure 4: The observed and expected 95% CL limits on the production cross-section times the Higgs decay branching ratio as a function of m_H for the $ZH \to \nu\bar{\nu}b\bar{b}$ channel. The liimts are compared with the SM prediction.

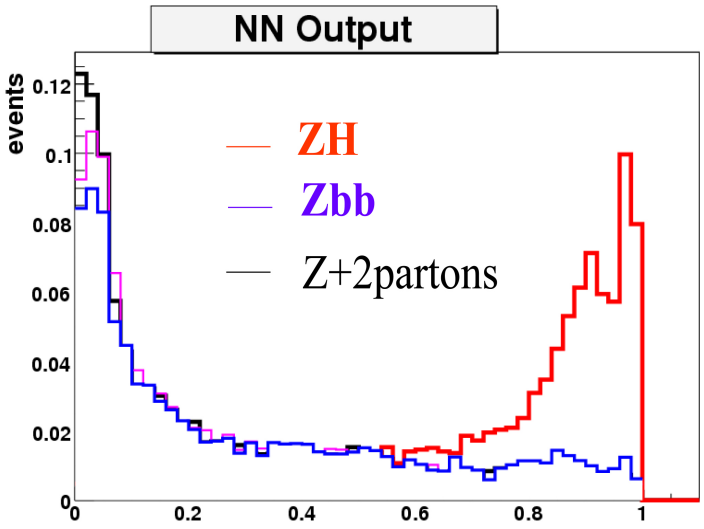

Figure 5: The distribution of the neural net discriminant function for the $ZH \to \ell^+\ell^- b\bar{b}$ channel, shown separately for the signal and for the major backgrounds, $Zb\bar{b}$ and $Z + 2$ partons. The data in this channel are still blind.

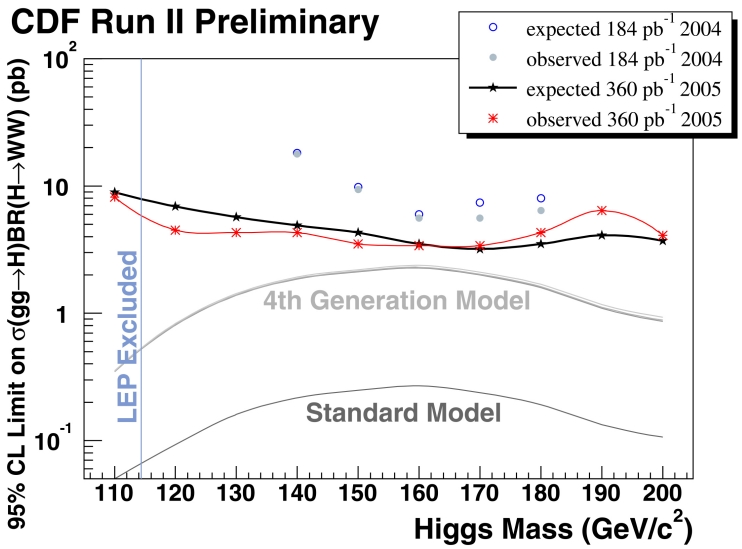

Figure 6: The observed and expected 95% CL limits on the production cross-section times the Higgs decay branching ratio as a function of m_H for the $gg \to H \to W^+W^-$ channel. The limits are compared with the SM prediction, and also the prediction of a model with a heavy fourth generation of SM-like fermions.

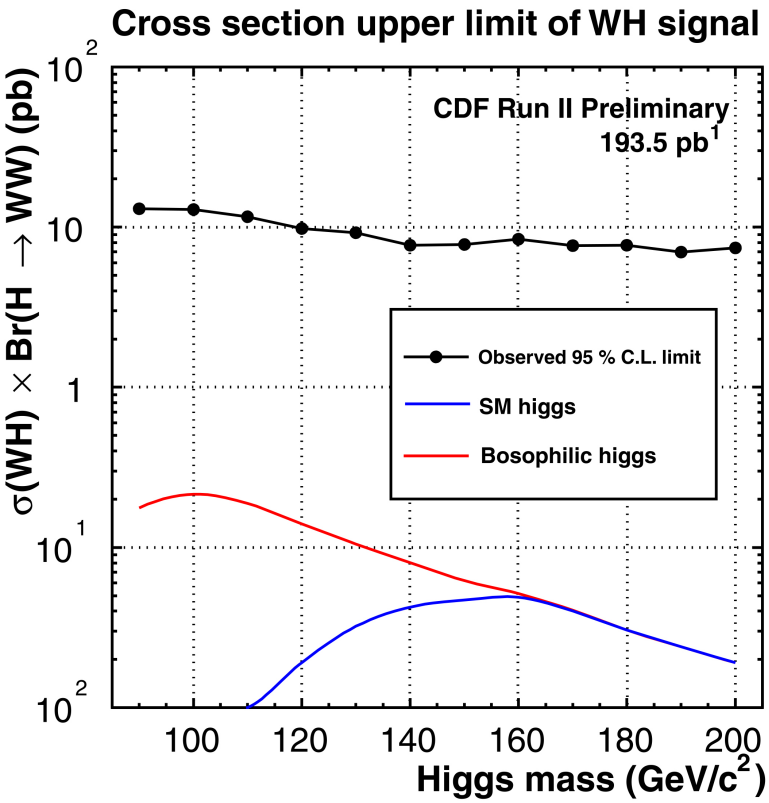

Figure 7: The observed 95% CL limit on the production cross-section times the Higgs decay branching ratio as a function of m_H for the $W^{\pm}H \rightarrow W^{\pm}W^{+}W^{-}$ channel. The limits are compared with the SM prediction, and also the prediction of a "bosophilic" (also known as "fermiophobic") model.

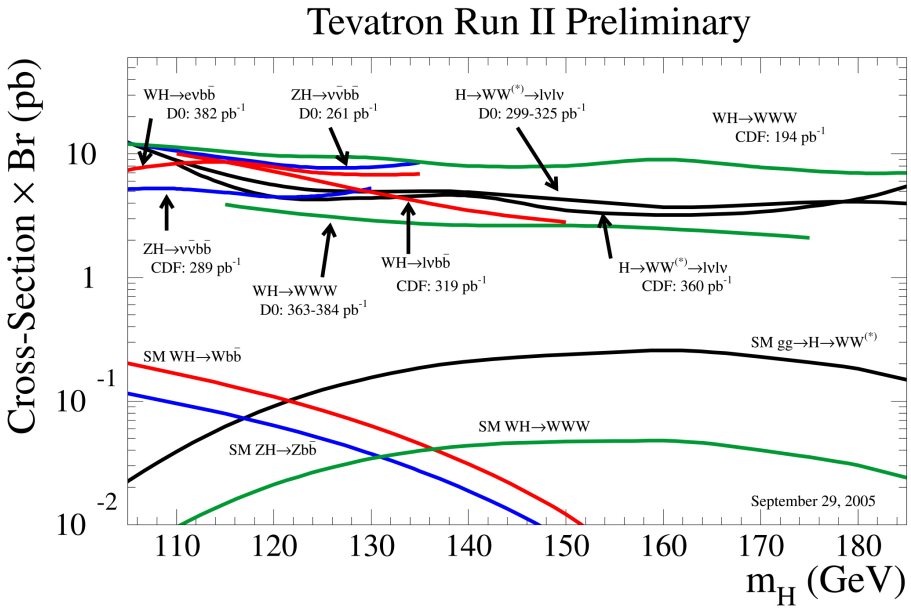

Figure 8: The observed 95% CL limits on the production cross section times the Higgs decay branching ratio for each of the five search channels, compared with DØ's limits, and also compared with SM expectations.

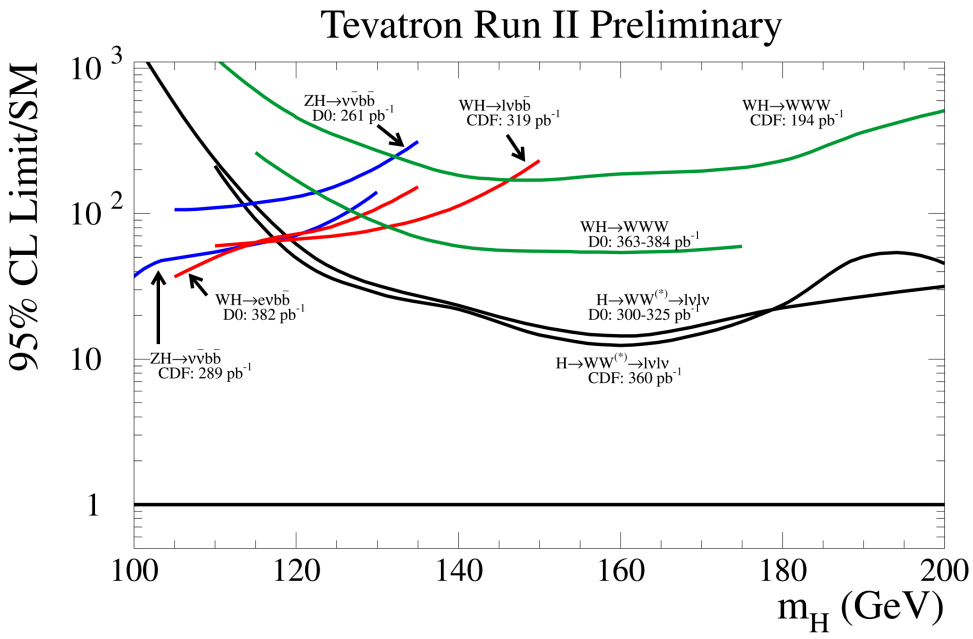

Figure 9: CDF and DØ's observed 95% CL limits on the production cross section times the Higgs decay branching ratio, divided by the corresponding SM predictions, for each of the five search channels.

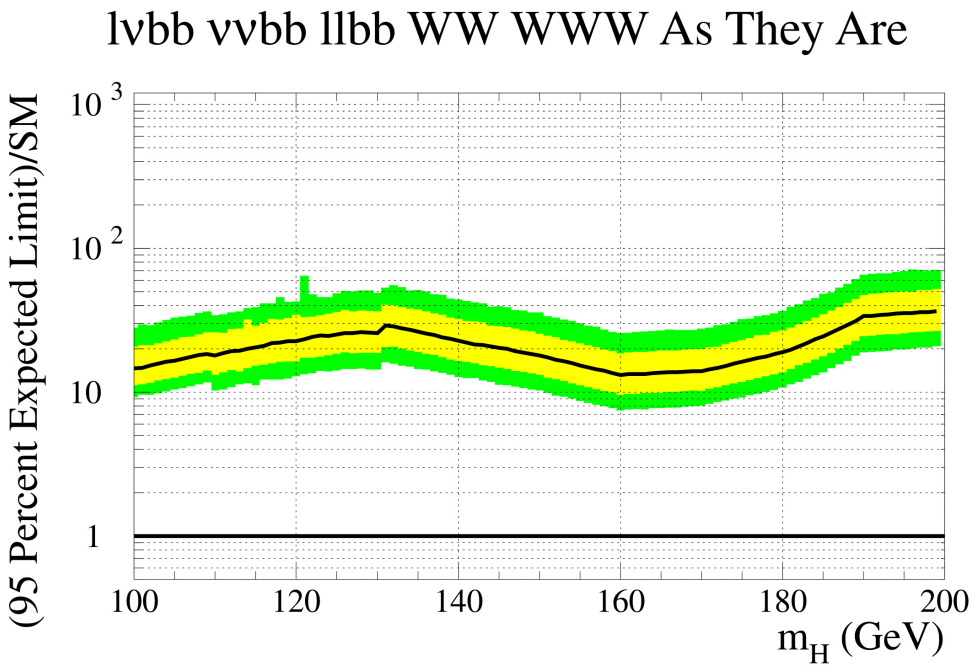

Figure 10: The expected 95% CL limit on the multiplicative scale factor of SM Higgs boson production for CDF's five SM Higgs boson search channels combined, as a function of m_H, assuming the absence of a Higgs boson. The yellow and green bands show the $\pm 1\sigma$ and $\pm 2\sigma$ expectations, which fluctuate depending on the possible data which may be observed.

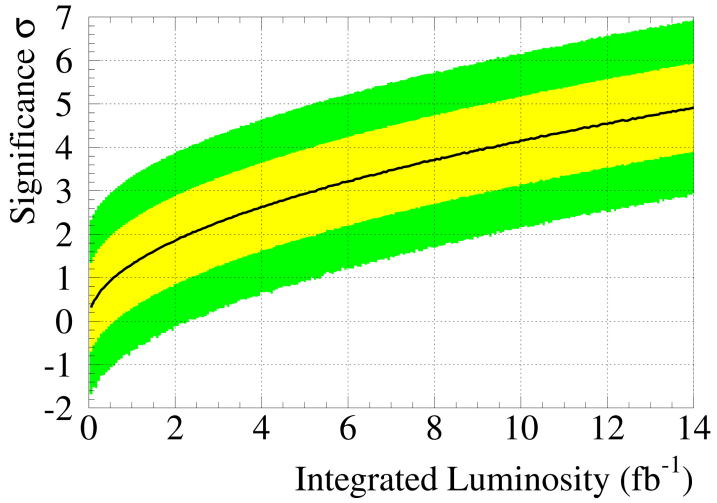

Figure 11: The evolution of the expected significance of an excess in the data if a Standard Model Higgs boson is present with a mass of 115 GeV. The yellow (light) interior band shows the $\pm 1\sigma$ distribution of the expected significance, and the green (darker) exterior band shows the $\pm 2\sigma$ range around the expectation. CDF and DØ are combined, and the foreseen sensitivity improvements have been assumed. The integrated luminosity is per experiment.

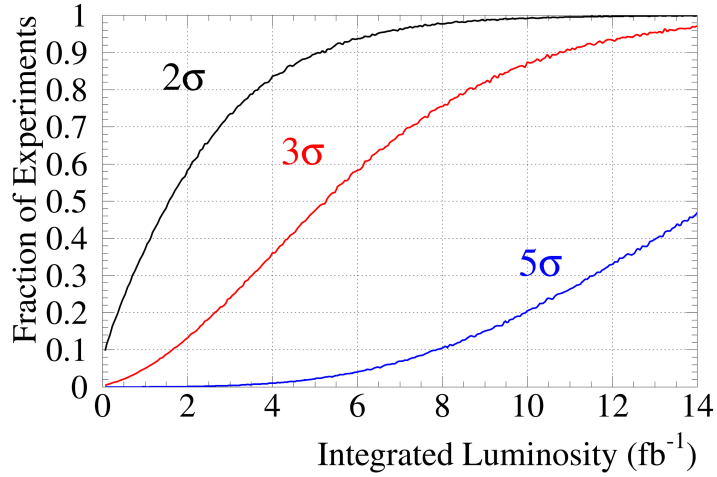

Figure 12: The fraction of experiments expected to make an observation of a 115 GeV SM Higgs boson if it is truly there, as a function of the integrated luminosity. CDF and DØ are combined, and the foreseen sensitivity improvements have been assumed. Separate curves are shown for the fraction of experiments observing a $\geq 2\sigma$ excess in the data, a $\geq 3\sigma$ excess, or a $\geq 5\sigma$ excess.

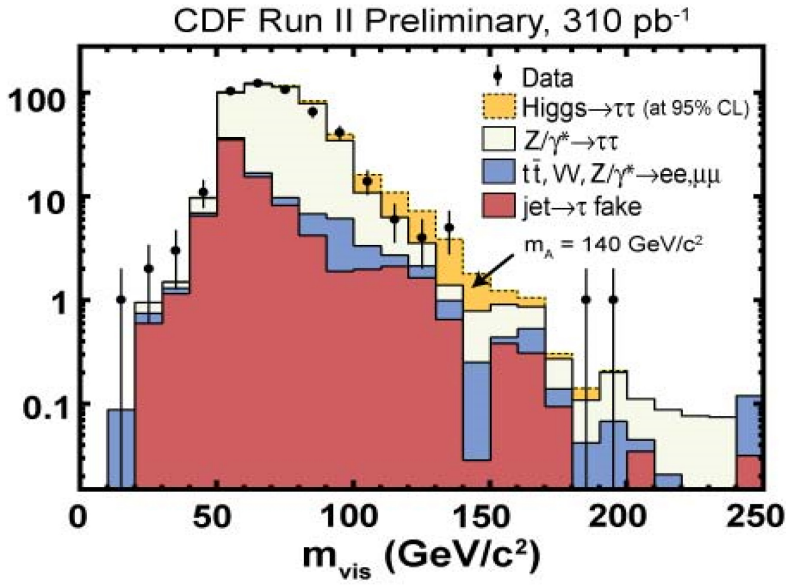

Figure 13: The invariant mass of the reconstructed tau decay products in the MSSM $H \to \tau^+\tau^-$ search. The data (points) are compared to a sum of background predictions. A Higgs boson signal of mass $m_A = 140$ GeV, with a production cross section just at the exclusion threshold, is shown.

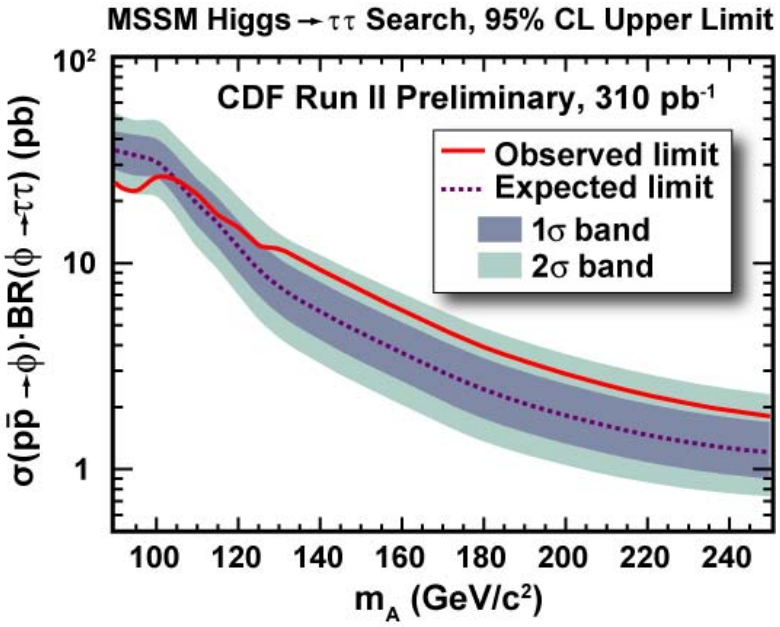

Figure 14: The 95% CL limit on the production cross section times the decay branching ratio for Higgs bosons decaying to tau pairs, using 310 pb^{-1} of CDF data, as a function of the Higgs boson mass.

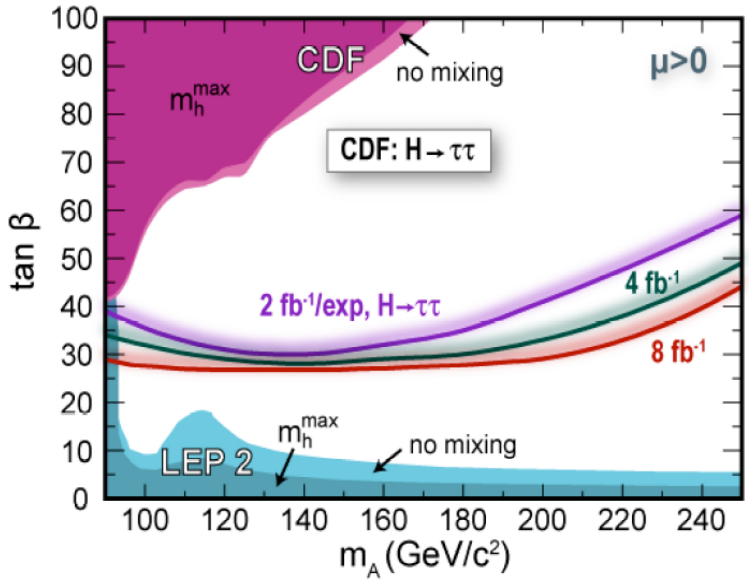

Figure 15: The observed 95% CL limits in the tau channel in the $(m_A, \tan\beta)$ plane, for the m_H-max MSSM benchmark scenerio and also the no-mixing benchmark scenario, using 310 pb^{-1} of CDF data. Projections are shown for the expected combined CDF+DØ exclusion reach for 2, 4, and 8 fb^{-1} per experiment.